Orientation-dependent optic-fiber accelerometer based on excessively tilted fiber grating

LANG XIE,[1] BINBIN LUO,[1,2,*] MINGFU ZHAO,[1] OU DENG,[1] ENHUA LIU,[1] PENG LIU,[1] YAJIE WANG,[1] AND LIN ZHANG[2]

[1]Chongqing Key Laboratory of Optical Fiber Sensor and Photoelectric Detection, Chongqing University of Technology, Chongqing 400054, China
[2]Aston Institute of Photonic Technologies (AIPT), Aston University, Birmingham B4 7ET, UK
*Corresponding author: luobinbin@cqut.edu.cn

Received 08 Month 2019; revised 11 Month, 2019; accepted XX Month XXXX; posted XX Month XXXX (Doc. ID XXXXX); published XX Month XXXX

An orientation-dependent optic-fiber accelerometer based on the excessively tilted fiber grating (ExTFG) inscribed in SM28 fiber is demonstrated, which is based on the optical power demodulation scheme. Without any complicated processing, the cladding mode resonances of the bare ExTFG show high sensitivity to slight perturbation of bending. Due to its excellent azimuth-related bending properties, such a bare ExTFG fixed on a simple cantilever beam has exhibited strong orientation-dependent vibration properties. Experiment results show that TE mode of the sensor can provide a maximal acceleration sensitivity of 74.14 mV/g @72 Hz and maximal orientation sensitivity of 9.1 mV/deg, while for TM mode, a maximal acceleration sensitivity of 57.85 mV/g @72 Hz and maximal orientation sensitivity of 7.4 mV/deg could be achieved. These unique properties would enable the sensor acts as a vector accelerometer for the applications in many vibration measurement fields.

http://dx.doi.org/10.1364/OL.99.099999

Vibration (acceleration) monitoring and detection are extremely important for engineering structural health, geological prospecting, space flight and aviation, and so on [1-3]. Compared with traditional vibration accelerometers based on piezoelectric or micro-electromechanical systems (MEMS), optic-fiber based sensing techniques possess the advantages including high sensitivity, compact size, immunization to electromagnetic, remote sensing and resistance to hash environment. In the past decades, many types of optical fiber vibration accelerometer have been proposed, such as the wavelength-demodulation vibration sensors utilizing diaphragm integrated FBG [4-6], phase-demodulation vibration sensors [7-9], distributed Bragg reflector (DBR) fiber laser accelerometer [10] and distributed vibration sensing [11], etc. However, many of these optic-fiber accelerometers are scalar sensors. Generally speaking, vibration is a vector parameter which contains not only amplitude but also direction information. Therefore, it is important to detect both the amplitude and orientation of vibration. To date, several optic-fiber based vector vibration sensors have been developed. Zhang [12] using polarized maintain fiber (PMF) to design an acceleration sensor based on modal interferometer, which could provide a very high sensitivity of 75.04 mrad/g below 180 Hz. However, the orientation properties of vibration sensing are not satisfied and strongly depended on the coil effect of PMF on the acrylonitrile-butadiene-styrene (ABS) disk. Guo presented vector vibration sensors based on tilted fiber Bragg grating (TFBG) with special designed structures including TFBG combined with an abrupt biconical taper [13], multi-mode TFBG spliced to single-mode fiber [14] and TFBG inscribed in depressed cladding fibers [15, 16]. By utilizing the polarization dependence properties of cladding modes of TFBG, the amplitude and orientation of vibration simultaneously measured by optical power demodulation scheme were realized. Although the intrinsic polarization dependence properties of TFBG could benefit the measurement for the vibration orientation, the special designed structures would complicate the process of fabrication and increase costs. Therefore, it is essential to design a vibration sensor possessing the advantages of vector monitoring, simple structure, high sensitivity and reproducibility.

Excessively tilted fiber grating (ExTFGs) were first reported by Zhou [17] in 2006, which have a tilt angle of ~81° and a relatively long grating pitch (~28 μm), thus it can couple core mode to the co-propagating cladding modes. Due to the remarkable birefringence induced by the excessively tilt fringe in the fiber core, ExTFGs could produce dual-peaks corresponding to orthogonal polarization dependent modes (i.e., TE and TM) for each coupling mode [18, 19]. The initial interval of dual-peaks of the ExTFG is usually 4~7 nm, and the excellent polarization-related property permits the sensor to be applied as twisting [20], transverse loading [21] and vector magnetic field sensors [22]. Besides, ExTFGs have very low temperature sensitivity (~5 pm/°C) [18], which would assure the salability in applications. In the experiment, we find that ExTFGs have azimuth-dependent bending sensitivities, thus it can be utilized to achieve measurement of vector vibration. In this paper,

we report an orientation-dependent optic-fiber accelerometer based on the bare ExTFG fixed on a simple cantilever beam, which can realize both the amplitude [23] and orientation measurement of the vibration by using optical power demodulation method.

The ExTFGs (tilt angle 81°, length 10 mm) were provided by Aston Institute of Photonic Technologies, Aston university, UK. The transmission spectra of ExTFGs in the 1450~1650 nm band and the polarization dependence spectra close to 1550 nm are shown in Figs. 1(a) and (b), respectively. The configuration of the ExTFG based vector acceleration sensor is shown in Fig. 1(c), where the fast axis and slow axis of the ExTFG have been marked. For convenience of analysis, in this study, we define the vibration (or bending) orientation as the intersection angle between the vibration (or bending) plane and the fast axis (i. e., direction of TE mode).

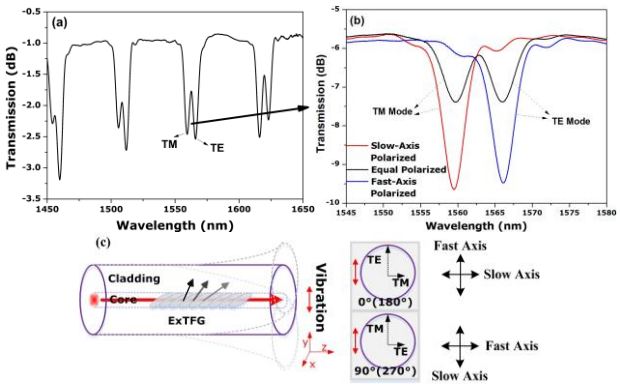

Fig. 1. (a) Transmission spectrum of the ExTFG from 1450 nm to 1650 nm; (b) Polarization dependence spectra at the C/L band (red is the TM mode corresponding to slow axis; blue is the TE mode corresponding to fast axis; black is the un-polarized light with TE and TM mode equally exited); (c) Schematic diagram of the ExTFG based vector acceleration sensor (left: profile view; right: cross-section view).

Before fixed on the cantilever beam, the axis strain and vector bending performances of the ExTFG were evaluated. As shown in Fig. 2, the axis strain sensitivities of TE and TM mode is -2.93 pm/με and -2.31 pm/με, respectively. Obviously, the axis strain sensitivity of TE mode is larger than that of TM mode, this is in consistent with the results reported by Zhou [17], the coefficient is negative; i.e., the resonant peak moves to the shorter-wavelength side. Besides, we find that axis strain sensitivities are independent of the orientation.

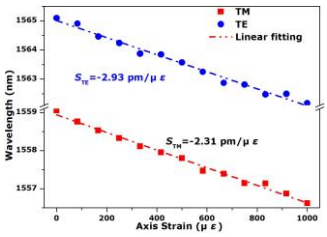

Fig. 2. Wavelength shift as the variation of axis strain of the ExTFG.

Figs. 3(a)-(d) are the spectral evolutions of TE mode as the bending curvature varying from 0 m^{-1} to 0.575 m^{-1} for the bending orientation of 0°, 90°, 180°and 270°, respectively, revealing that the bending response of TE mode is much better when the fast axis and the bending orientation are in parallel (0° or 180°) as compared with the case of being perpendicular (90° or 270°). This is reasonable because that the maximum structural deformation induced by the fiber bend is in the bending plane, which would lead to a relatively larger changes in the effective index difference between the core mode and cladding modes as well as in grating pitch in this plane.

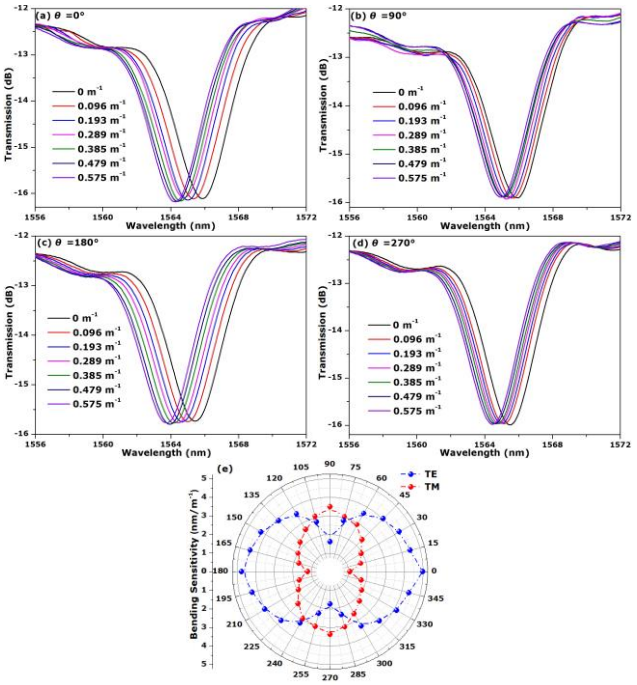

Fig. 3. Spectral evolutions of TE mode of the ExTFG as bending curvature varying from 0 to 0.575 m^{-1} for the bending orientation of (a) 0°, (b) 90°, (c) 180°, and (d) 270°. (e) Bending sensitivity as a function of orientation for TE and TM mode in polar coordinate system.

For inspecting the orientation bending properties of the ExTFG, we calibrated the bending sensitivities of TE and TM mode by adjusting the bending orientation from 0° to 360° with an increment of 15°, the results are illustrated as polar coordinate system in Fig. 3(e). It can be seen that both the bending sensitivities of TE and TM mode have very good orientation dependence and exhibit an "8" shape perpendicular to each other. Therefore, when the fast axis of ExTFG is parallel to the bending plane, the bending sensitivity of TE mode would achieve its maximal value while the TM mode depressed to its minimal value, and vice versa. These polarization evolution trends are in accordance with our theoretical prediction. More specifically, according to the calibrated results in Fig. 3(e), the bending sensitivities of TE mode are -4.981 nm/m^{-1} (@0°) and -4.752 nm/m^{-1} (@180°) in the parallel plane, while in the perpendicular plane are -1.617 nm/m^{-1} (@90°) and -1.735 nm/m^{-1} (@270°), and the orientation sensitivity for TE mode could reach -34.6 pm/(m^{-1}·deg); The bending sensitivities of TM mode are -3.486 nm/m^{-1} (@90°) and -3.372 nm/m^{-1} (@270°) in the parallel plane, whereas in the perpendicular plane are -1.076 nm/m^{-1} (@0°) and -1.203 nm/m^{-1} (@180°), and its maximal orientation sensitivity is -25.8 pm/(m^{-1}·deg). Therefore, the bending responses of TE mode are better than those of TM mode, for both the amplitude and

orientation. Utilizing the excellent azimuth-related bending properties, we could design the ExTFG vector vibration sensor.

The experimental setup (same as Ref. 23) for the vector accelerometer is shown in Fig. 4(a), including a tunable narrow-band laser source (TLS, 196.25~186.35 THz, ±0.5 GHz, line width < 100 kHz), polarizer, polarization controller (PC), Piezoelectric ceramic (PZT) and its amplifier, cantilever beam, ExTFG, optical fiber rotators, photoelectric detection (PD) and oscilloscope. The polarization direction of the linearly polarized light was controlled by PC, so as to tune the ExTFG to work on TE mode, TM mode or equal excitation of TE/TM mode. The ExTFG was fixed on the cantilever beam made of brass with thickness of 0.3 mm, and the ends of ExTFG were rotated by a pair of optical fiber rotators to precisely adjust the orientation of the fast axis. Vibration produced by PZT caused bending deformation of the cantilever beam, which would result in the axis and bending strain of the ExTFG.

According to our previous study, the spectrum would undergo not only the linear shift in the resonance wavelength but also monotonic changes in the optical power when the ExTFG under the axis strain and bending strain simultaneously, as illustrated in Fig. 4(b). Besides, the optical power changes at the 3dB point (FHMW) of the spectrum have the maximal gradient as well as the best SNR under a certain vibration amplitude as compared with other wavelength point. Therefore, in the subsequent vibration sensing experiments, the wavelength of the narrow-band light was fixed at the 3dB point of TE (or TM) mode, the optical power modulated with vibration was detected by PD, which was output to the oscilloscope for real-time monitoring.

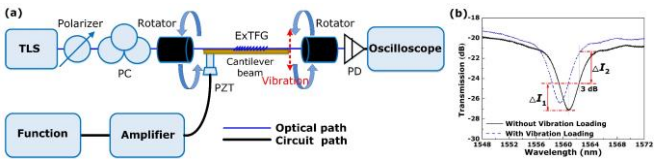

Fig. 4. (a) Setups of the vector vibration sensing system; (b) The optical power demodulation principle of the ExTFG based vibration sensor.

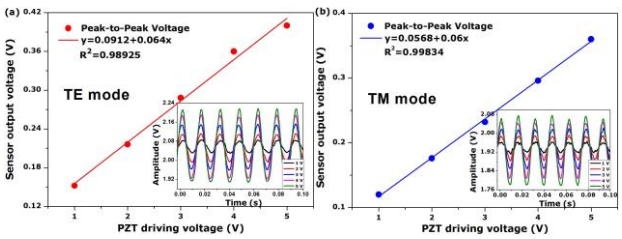

Fig. 5. Output voltage of the sensing system for (a) TE mode and (b) TM mode in a random vibration orientation under 65Hz. Insets show the corresponding waveform responses in time domain.

The used PZT has a flat amplitude-frequency response in the range from 10Hz to 350Hz and a linear acceleration response to the PZT driving voltage at a fixed frequency; the designed cantilever beam has an inherent resonant frequency of 72Hz. Figs. 5(a) and (b) are the output voltages (peak-to-peak voltage) of the vibration sensing system working at 65 Hz (a general frequency rather than resonant frequency of the cantilever beam) when TE and TM mode of the ExTFG are in a random orientation, respectively, demonstrating that the sensing system has a good linear response to the acceleration amplitude.

We now demonstrate that the amplitude and orientation information of vibration can be obtained simultaneously by a simple optical power measurement of the TE or TM mode. In the experiment, we rotated the ExTFG from 0° to 360° with a 15° increment by the optical fiber rotators. Two sets of experiment with driving voltages of 3 V and 5 V at 72 Hz were conducted for TE and TM mode, respectively. During the sensing process, the spectrum of the ExTFG was adjusted by the PC to its initial spectrum (that in the first vibration experiment) after each rotation, so as to eliminate the effect of twist on light polarization, thus ensuring the reliability of orientation-dependent experiments. The TE mode of the ExTFG is firstly used for the analysis. The left of Figs. 6(a), (b) and (c) are the Fast Fourier transform (FFT) of the output signals of TE mode when the fast axis of the ExTFG is oriented at 0°, 45° and 90°, respectively, and insets show the corresponding waveform responses in time domain (blue: 5 V and red: 3 V). It can be seen from the figures that the output voltage (peak-to-peak voltage) can achieve its maximum when the fast axis is parallel to vibration direction (@ 0°) and reach the minimum at vertical direction (@ 90°), presenting good orientation-dependent property for the ExTFG vibration sensor. The responses of TM mode are also shown in the right of Figs. 6(a)-(c), indeed, TM mode has similar orientation-dependent properties to the TE mode. Therefore, taking the above results (Fig. 5 and Fig. 6) into consideration, we can confirm that the output of the ExTFG is linearly increasing with the acceleration amplitude at a certain orientation and, more importantly, it is highly angle dependence, which agrees well with our expectation.

Besides, the specific FFT results of Figs. 6(a)-(c) are showed in Fig. 6(d), indicating that the SNRs of TE mode are 44.3 dB, 44.2 dB and 35.1 dB for the oriented angle of 0°, 45°and 90°, respectively, when the driving voltage is 5 V. While for the case of 3 V, they are 43.9 dB, 42.3 dB and 32.5 dB, respectively, which are slight lower than those of the former. Therefore, the SNR of TE mode is significantly related to the vibration orientation, it would be the best when the fast axis coincides with vibration direction, and quickly declines as it becomes more and more close to the slow axis direction. We can see from Figs. 6(a)-(c) that there are many high-order harmonics, this is due to the fact that we did not wrap the whole sensor on the surface of the cantilever beam but only fix its two ends for the convenience of rotating fiber in the experiments. However, if we adopted the former packing method, this situation would be well eliminated without affecting the performance of the sensor. With the same procedures, the output signals of TM mode under 3 V and 5 V are also analyzed and shown in Fig. 6(d), manifesting that the above SNR properties of TE mode are suitable for TM mode as well.

Considering the precalibrated linear relation between acceleration amplitude and driving voltage at the inherent resonance frequency (72 Hz) of the cantilever beam, the acceleration sensitivities for TE and TM mode at different vibration orientation could be calculated by using the output (peak-to-peak voltage) of the vibration sensing system, the results are plotted in the polar coordinate system as shown in Fig. 6(e). We can see that, similar to the vector bending properties in Fig. 3(e), the acceleration sensitivities of TE and TM mode are highly orientation dependent and exhibit "8" shapes perpendicular to each other. These results suggest that the vector vibration responses of the ExTFG are mainly induced by the orientation properties of its bending effect, which is

originated from its birefringence caused by the asymmetric structure of the grating.

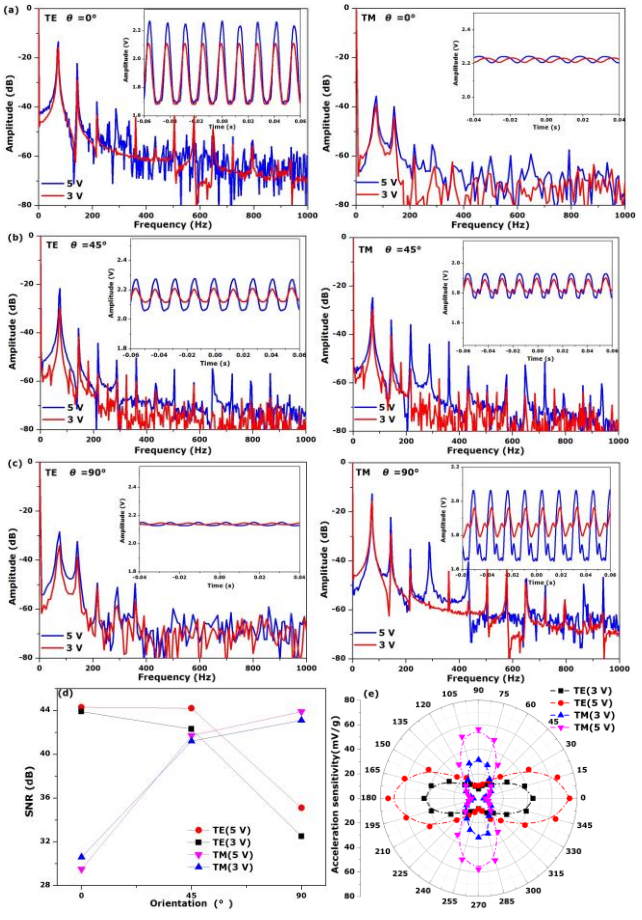

Fig. 6. (a)-(c) Frequency domain response diagrams of TE (left) and TM (right) modes @72 Hz under fixed driving voltages of 5 V (blue) and 3 V (red) with oriented angle of 0°, 45°and 90°, respectively. Insets show the corresponding waveform responses in time domain. (d) The corresponding SNR for TE and TM modes; (e) Acceleration sensitivity as function of vibration orientation for TE and TM modes @72 Hz in polar coordinate system under fixed driving voltages of 5 V and 3 V.

The acceleration sensitivities of TE and TM modes as the driving voltage at 5 V and 3 V are both characterized in Fig. 6(e). According to Fig. 6(e), TE mode of the ExTFG can provide the maximal acceleration sensitivity and maximal orientation sensitivity of 74.14 mV/g and 9.1 mV/deg under 5 V, respectively, and 44.34 mV/g and 5.1 mV/deg under 3 V, respectively. While for the TM mode, it can provide the maximal acceleration sensitivity and maximal orientation sensitivity of 57.85 mV/g and 7.4 mV/deg under 5 V, respectively, and 31.87 mV/g and 3.7 mV/deg under 3 V, respectively. Obviously, both the response and orientation dependence of TE mode are much better than those of TM mode under the same condition, it is because that the intrinsic axis strain sensitivity and bending sensitivity of TE mode are higher than those of TM mode. Furthermore, the higher acceleration amplitude (PZT driving voltage), the stronger orientation dependence of TE and TM modes. In general, the above phenomena are in good consistent with our previous analysis.

An orientation-dependent optic-fiber accelerometer based on an ExTFG fixed on a simple cantilever beam is presented. By utilizing the excellent azimuth-dependent bending sensitivity of ExTFG, the sensor shows superior performances with the sensing capability of vibration orientation and amplitude. Experimental results confirm that the maximal acceleration sensitivity and orientation sensitivity of the sensor could achieve 74.14 mV/g and 9.1 mV/deg, respectively. Moreover, the proposed accelerometer owns the advantages of compact structure, easy fabrication, simple demodulation, which have great potentiality to be applied as vector accelerometer in many vibration measurement fields.

Funding. This work was supported by the National Natural Science Foundation of China (NSFC) (61875026, 61505017).

References

1. G. Kocharyan, A. Ostapchuk, and D. Pavlov, Sci. Rep. **8,** 10764 (2018).
2. M. Dilena, A. Morassi, Mech. Syst. Signal Process. **25,** 1485 (2011).
3. I. Trendafilova, M. Cartmell, W. Ostachowicz, J. Sound Vib. **313,** 560 (2008).
4. Q. P. Liu, X. G. Qiao, Z. A. Jia, H. W. Fu, H. Gao, and D. K. Yu, IEEE Sens. J. **14,** 1499 (2014).
5. M. Fabian, D. Hind, C. Gerada, T. Sun, and K. Grattan, J. Lightwave Technol. **36,** 1046 (2018).
6. F.X. Zhang, C. Wang, X. L. Zhang, S. D. Jiang, J. S. Ni, and G. D. Peng, Chinese Opt. Lett., **17**, 010601 (2019).
7. W. Wang, Y. D. Shen, T. Guo, X. G. Qiao, and Q. Z. Rong, Appl. Opt. **58**, 5852 (2019).
8. J. Y. Wang, F. Ai, Q. Z. Sun, T. Liu, H. Li, Z. J. Yan, and D. M. Liu, Opt. Express **26,** 25293 (2018).
9. J. Ma, Y. Q. Yu, and W. Jin, Opt. Express **23**, 29268 (2015).
10. T. Liu, J. W. Cheng, D. D. Lv, Y. Y. Luo, Z. J. Yan, K. Wang, C. Q. Li, D. M. Liu, and Q. Z. Sun, J. Lightwave Technol. **37**, 2946 (2019).
11. Z. N. Wang, J. J. Zeng, J. Li, Q. Fan, H. Wu, F. Peng, L. Zhang, Y. Zhou, and Y. J. Rao, Opt. Lett. **39**, 5866 (2014).
12. G. Zhang, X. Q. Wu, Q. Ge, S. L. Li, J. H. Shi, W. Liu, C. Zuo, and B. L. Yu, Appl. Opt. **58**, 3945 (2019).
13. T. Guo, L. Y. Shao, H. Y. Tam, P. A. Krug, and J. Albert, Opt. Express **17,** 20651 (2009).
14. T. Guo, L. B. Shang, Y. Ran, B. O. Guan, and J. Albert, Opt. Lett. **37,** 2703 (2012).
15. S. S. Cai, Y. G. Nan, W. P. Xie, J. Yi, X. Y. Chen, Q. Z. Rong, H. Liang, M. Nie, G.D. Peng, and T. Guo, IEEE Photon. Technol. Lett. **29,** 2171 (2017).
16. Q. Z. Rong, T. Guo, W. J. Bao, Z. H. Shao, G. D. Peng, and X. G. Qiao, Sci. Rep. **7,** 11856 (2017).
17. K. M. Zhou, L. Zhang, X. F. Chen, and I. Bennion, Opt. Lett. **31,** 1193 (2006).
18. Z. J. Yan, Q. Z. Sun, C. L. Wang, Z. Y. Sun, C. B. Mou, K. M. Zhou, D. M. Liu, and L. Zhang, Opt. Express **25,** 3336 (2017).
19. G. L. Yin, S.Q. Lou, Q. Li, and H. Zou, Opt. Laser Technol. **48,** 60 (2013).
20. X. F. Chen, K. M. Zhou, L. Zhang, and I. Bennion, IEEE Photon. Technol. Lett. **18,** 2596 (2006).
21. R. Suo, X. F. Chen, K. M. Zhou, L. Zhang, and I. Bennion, Meas. Sci. Technol. **20,** 034015 (2009).
22. T. A. Lu, Y. Z. Sun, Y. Moreno, Q. Z. Sun, K. M. Zhou, H. S. Wang, D. M. Liu, L. Zhang, and Z. J. Yan, Opt. Lett. **44,** 2494 (2019).
23. B. B. Luo, W. M. Yang, X. Y. Hu, H. F. Lu, S. H. Shi, M. F. Zhao, L. Ye, L. Xie, Z. Y. Sun, and L. Zhang, Appl. Opt. **57,** 2128 (2018).